Thermoelectric power of $La_{1-x}Ca_xMnO_{3+\delta}$: Inadequacy of the nominal $Mn^{3+/4+}$ valence approach

M. F. Hundley and J. J. Neumeier
Materials Science and Technology Division, Los Alamos National Laboratory, Los Alamos, New Mexico 87545
(Received 25 November 1996)

The temperature-dependent thermoelectric power (TEP) and resistivity of $La_{1-x}Ca_xMnO_{3+\delta}$ polycrystals ($0 \leqslant x \leqslant 0.45$) are reported. The TEP data are analyzed within an adiabatic small polaron description in order to determine the number of charge carriers per active transport site in the paramagnetic state. The TEP in the small-polaron regime above T_C is significantly smaller than that predicted by nominal $Mn^{3+/4+}$ valence arguments. This indicates that more holelike charge carriers and/or fewer accessible Mn transport sites are present in these compounds than expected based on the divalent doping levels employed. This result is consistent with a substantial degree of $3d^4$-$3d^4$ (Mn^{3+}-Mn^{3+}) charge disproportionation into more stable $3d^5$-$3d^3$ (Mn^{2+}-Mn^{4+}) pairs. [S0163-1829(97)06617-4]

The electronic transport and magnetic properties of the doped ferromagnetic (FM) semiconductors $La_{1-x}A_xMnO_{3+\delta}$ (A=Ba, Ca, or Sr) were first examined many years ago.[1] Undoped $LaMnO_3$ is an insulating superexchange antiferromagnet (AFM), while divalent substitution for La^{3+} leads to a mixed $Mn^{3+/4+}$ nominal valence, a FM ground state intimately associated with a metal-insulator (MI) transition at $T_{MI}=T_C$, and the colossal magnetoresistance[2] (CMR) effect. The concept of double exchange (DE) was proposed to account qualitatively for the close interplay between magnetic order and electronic transport in these compounds.[3] The recent rediscovery of the CMR effect[4] has led to renewed interest in these compounds with an emphasis on moving beyond the basic notions of DE in order to uncover the physical mechanisms involved in the CMR effect. The emerging theoretical picture is that DE alone cannot account for the physical behavior of the CMR system at other than a very crude level.[5] Instead, it may be that the CMR effect stems from an interplay between magnetic exchange and a strong electron-phonon interaction that occurs due to the Jahn-Teller (JT) active octahedrally coordinated $3d^4$ ions present in these materials.[5] In this scenario[6] the interplay between the spin, charge, and lattice degrees of freedom leads to localized small-polaron quasiparticles in the paramagnetic state, while long-range order delocalizes the carriers, leading to metalliclike large polaron transport below T_C. In support of this picture, experimental evidence[7] indicates that delocalized polaronlike effects persist below T_C.

Central to the above description is that divalent substitution for La^{3+} results in Mn mixed valency and that charge-carrier transport involves e_g holes on $3d^3$ (Mn^{4+}) sites hopping to e_g states on neighboring $3d^4$ (Mn^{3+}) sites. Thermoelectric power (TEP) measurements[8] are a powerful way to check for the validity of this description because the carrier contribution to the Seebeck coefficient S depends directly upon the fractional hole concentration c_h in polaronic systems. In this work we present temperature-dependent TEP measurements of polycrystalline $La_{1-x}Ca_xMnO_{3+\delta}$ samples synthesized in the range $0 \leqslant x \leqslant 0.45$. Our TEP results are fully consistent with metalliclike conduction below T_C and small-polaron quasiparticle hopping in the paramagnetic state. The magnitude of S in the small-polaron regime indicates that there are far more holes per active transport site than would be expected based on a simple nominal $Mn^{3+/4+}$ valence description. This may be an indication that charge disproportionation is present in this system due to the near degeneracy of Mn^{3+}-Mn^{3+} and Mn^{2+}-Mn^{4+} complexes in octahedrally coordinated systems.

Polycrystalline $La_{1-x}Ca_xMnO_{3+\delta}$ samples were synthesized by standard solid-state reactions; stoichiometric quantities of high-purity (99.99% or better) La_2O_3, $CaCO_3$, and MnO_2 powders underwent four grinding-firing stages at 1250 °C to 1400 °C. All samples were slow-cooled in air over a 20-h period except for the undoped specimen which was cooled in Ar to limit the uptake of excess oxygen. X-ray-diffraction measurements showed single-phase material in all cases. Iodometric titration (with the assumption that La, Ca, Mn, and O valences are +3, +2, +2, and −2 in acidic solution) was employed to determine the average Mn valence (and, in turn, the excess oxygen content) present in each preparation batch. T_C was determined from magnetization Arrott plot measurements (M^2 vs H/M) using a SQUID magnetometer. The resistivity ρ and TEP were determined on the same specimen for each Ca-doping level in the 4–325 K temperature range. Electrical resistivity measurements employed a conventional four-probe dc technique while TEP measurements were performed by suspending a sample between electrically isolated copper posts across which a variable temperature gradient was applied. The absolute TEP was determined relative to copper by a copper-constantan reference thermocouple. Electrical contacts were achieved with silver epoxy or paint. The stoichiometry, excess oxygen content, average Mn valence, T_C, and transport activation energies are presented in Table I for the seven samples considered here.

The resistivity and TEP for Ca-doped samples with doping levels ranging from $x=0$ to 0.45 are shown in Fig. 1 (data at $x=0.33$ and 0.45 are omitted for clarity). We focus first on the 21% Ca-doped specimen. In this sample magnetization measurements indicate that magnetic order occurs at

TABLE I. Stoichiometry for the $La_{1-x}Ca_xMnO_{3+\delta}$ samples employed in the TEP study; $x+2\delta$ is the average Mn valence, T_C is the Curie temperature, and E_ρ and E_S are the $T>T_C$ activation energies as determined from resistivity and TEP measurements, respectively.

x	δ ($\pm$ 0.003)	$x+2\delta$	T_C (K) ($\pm$ 5)	E_ρ (meV) ($\pm$ 5)	E_S (meV) ($\pm$ 2)
0	0.013	0.026	–	215	33
0.18	0.03	0.24	170	134	27
0.21	0.017	0.244	205	131	19
0.25	0.03	0.31	230	128	15
0.33	0.03	0.39	271	81	2
0.40	0	0.40	270	62	2
0.45	0.013	0.476	252	50	1

the same temperature where ρ peaks (205 K), while S peaks roughly 20 K above T_C. The abrupt drop in both ρ and S near T_C is fully consistent with carrier delocalization (i.e., a substantial mobility increase) due to the onset of long-range magnetic order. The few-μV value of S well below T_C is typical for metalliclike materials. For $T>T_C$ the T dependence of both ρ and S are described by

$$\rho(T)=\rho_0 T\exp\left(\frac{E_\rho}{k_B T}\right) \quad (E_\rho=131\ \text{meV}) \tag{1}$$

and

$$S(T)=\left(\frac{k_B}{e}\right)\left(\alpha+\frac{E_S}{k_B T}\right) \quad (E_S=19\ \text{meV}), \tag{2}$$

respectively, where k_B is Boltzmann's constant, e is the electron's charge, and α is a sample-dependent constant. The

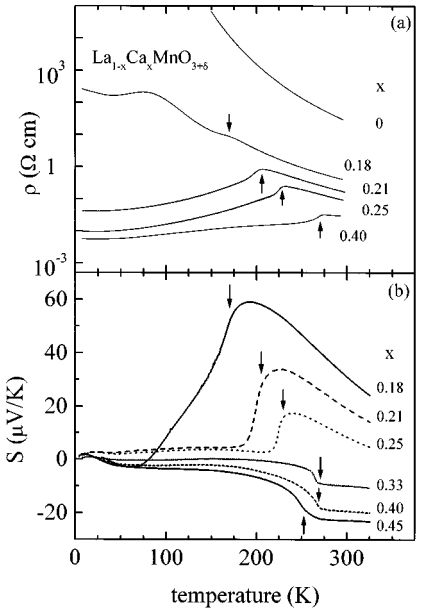

FIG. 1. The T-dependent resistivity (a) and Seebeck coefficient (b) for $La_{1-x}Ca_xMnO_{3+\delta}$ samples with varying Ca^{2+}-doping concentrations. The arrows indicate the magnetic ordering temperature for each specimen.

nature of Eqs. (1) and (2) indicates that in $La_{0.79}Ca_{0.21}MnO_{3.017}$ carrier transport involves adiabatic small-polaron hopping.[9] The large difference between E_ρ and E_S signifies that conventional band transport does not occur above T_C, but rather is the hallmark of small polaron hopping wherein the transport is dominated by temperature-dependent mobility effects.[9,10]

The same overall T-dependent trends evident in the 21% data are also present in the transport data for the other samples. For $LaMnO_3$ (not shown) no FM ordering occurs, and S is roughly 300 μV/K at 180 K and drops with increasing temperature. The $x=18\%$ sample is very close to the FM insulator-FM metal phase boundary;[1] although ρ exhibits only a weak anomaly at T_C for this doping level, full FM order is evident in magnetization measurements ($T_C=170$ K) and S displays a drop below T_C. The close proximity of this specimen to the FM-AFM phase boundary may be the reason for the presence of a second feature in ρ near 80 K and the very gradual nature of the drop in S below T_C. With increasing doping, ρ and S progressively decrease in value, while T_C reaches a maximum value (271 K) at 1/3 doping. E_ρ and E_S also decrease with increasing x (Table I). The large difference between these activation energies indicates that small polaron hopping occurs for all doping levels considered here. In all cases, S extrapolates to a high-temperature value of roughly $-20\,\mu$V/K. While the data in Fig. 1 are qualitatively similar to those reported previously,[8,10] we see no evidence for large low-temperature peaks in S that have been reported by Mahendiran *et al.*[11]

In order to determine the validity of various transport models, a quantitative analysis of the TEP data above T_C is needed. In small polar systems S is given by the sum of two terms,[12] a spin term S_σ, and charge-carrier term S_c. In the absence of magnetic order the spin term is a T-independent constant that is determined by the configurational entropy of placing a hole with spin σ_1 among sites with spin σ_0. The spin term is given by

$$S_\sigma=\left(\frac{k_B}{e}\right)\ln\left(\frac{2\sigma_1+1}{2\sigma_0+1}\right). \tag{3}$$

The strong Hund's rule exchange present in the manganites forces the spin of a hole on an e_g state to align with the t_{2g} electrons on the same Mn site. Hence, for a hole hopping amongst Mn^{3+} sites $\sigma_1=3/2$ and $\sigma_0=2$, leading to $S_\sigma=-19.2$ μV/K.[10] The presence of charge carriers produces a contribution to the TEP for low to moderate temperatures ($k_BT\leqslant E_S$) that is given by

$$S_c=\left(\frac{k_B}{e}\right)\left(\alpha+\frac{E_S}{k_B T}\right), \tag{4}$$

while at high temperatures ($k_BT\gg E_S$), S_c reaches a constant value given by the Heikes formula[13] (applicable due to the dominant Hund's rule exchange):

$$S_{c,\infty}=\left(\frac{k_B}{e}\right)\ln\left(\frac{1-c_h}{c_h}\right), \tag{5}$$

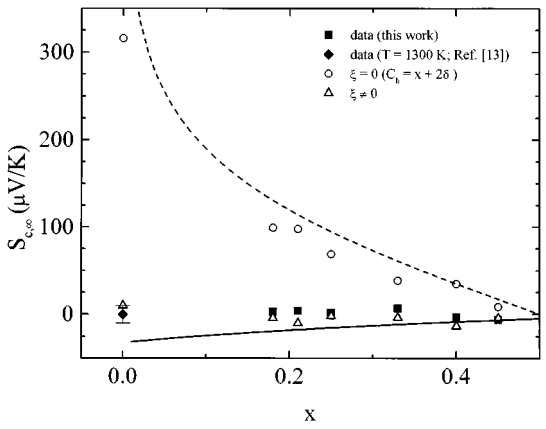

FIG. 2. Theoretical and experimental values of $S_{c,\infty}$ plotted vs Ca-doping concentration. Solid symbols are from experimental data, while the solid and dashed lines are produced from theoretical models with and without disproportionation, respectively (and, assuming $\delta=0$). The open symbols are the respective theoretical predictions when each sample's excess oxygen content is accounted for.

where c_h is the fractional hole concentration (number of holes per active transport site). When extrapolated to the high-T limit, S will obey the relation $S(\text{high-}T)=S_\sigma+S_{c,\infty}$. Hence, by extrapolating TEP data in this way one can directly determine the validity of transport models through their estimate of S_σ and $S_{c,\infty}(c_h)$.

An experimental estimate of $S_{c,\infty}$ can be made by extrapolating a_1+a_2/T fits[14] to $S(T>T_C)$ data and subtracting the expected spin-entropy contribution (-19.2 μV/K).[15] The experimental values for $S_{c,\infty}(x)$ are presented in Fig. 2. The $T\leqslant 325$ K data indicate that $S_{c,\infty}$ is 0 ± 20 μV/K for doping concentrations at and above 18%. High-T (1300 K) TEP measurements on $LaMnO_3$ (Ref. 16) indicate that this is also the case for undoped samples. This experimental result can be compared to that predicted by nominal $Mn^{3+/4+}$ valence arguments wherein every La^{3+} ion replaced by a Ca^{2+} ion converts one Mn^{3+} to Mn^{4+}. Similarly, each excess oxygen ion creates both cation vacancies[16] as well as converting two additional Mn ions to the 4+ state. If all Mn ions are active transport sites, the fractional hole concentration is $C_h=x+2\delta$. The dashed line in Fig. 2 gives the prediction for $S_{c,\infty}(x)$ based on this model assuming no excess oxygen ($\delta=0$); the prediction when the excess oxygen level for each specimen is accounted for corresponds to the open circles in Fig. 2. The wide difference between the data and the model predictions in Fig. 2 indicates that the TEP in the CMR compounds *is far too small to be explained by a simple nominal valence argument*. For example, with $c_h=0.3$ (valid for the $x=0.25$ sample) the Heikes expression predicts $S=54$ μV/K, far larger than the experimental value above T_C for any of the $x>0$ samples considered here.

The near-zero, doping-independent value of $S_{c,\infty}(x)$ indicates that $La_{1-x}Ca_xMnO_{3+\delta}$ behaves as if it were always half-filled ($c_h=1/2$) *regardless* of the divalent doping level. This suggests that there are far more holes present and/or far fewer active Mn transport sites than expected based on nominal valence arguments. Such behavior cannot be ascribed to the elimination of the JT splitting between e_g subbands brought on by increased divalent substitution;[17] that description would actually predict that the TEP would become severely electronlike [predicted TEP values include $S_{c,\infty}(x=0.25)=-44$ μV/K, $S_{c,\infty}(x=0.4)=-73$ μV/K], at odds with the results presented here. Similarly, the change in sign of the TEP near $x=0.3$ cannot be attributed to a crossover from holelike to electronlike transport at this doping level because this simplistic argument neglects the spin entropy contribution to the thermoelectric power.[11] An alternative approach to explain the half-filled nature of the TEP was recently proposed by Emin; the small polarons could be in a multiatomic state such that the only active Mn transport sites are those closely associated with a divalent dopant atom.[18] This model accounts for the discrepancy between the TEP data and the nominal valence picture by excluding a large fraction of the Mn ions from the transport process, although the reason for there being only two active transport states per divalent dopant (rather than one for each of the eight nearest Mn neighbors) needs to be more fully developed.

The TEP data can be reconciled with the electron configuration when the relative instability of the $3d^4$ (Mn^{3+}) configuration is considered. Thermal-gravinometric analysis (TGA) of high-temperature ($1000<T<1300$ K) excess-oxygen–oxygen-partial-pressure isotherms $\delta(T,P_{O2})$ (Ref. 16) are consistent with the presence of cation vacancies and Mn^{3+} charge disproportionation (CD) in both Ca- and Sr-doped lanthanum manganites; models based solely on excess oxygen leading to cation vacancies cannot account for the $\delta(T,P_{O2})$ data. Charge disproportionation ($2\ Mn^{3+}\rightarrow Mn^{2+}+Mn^{4+}$) is driven by the degeneracy of Mn^{3+}-Mn^{3+} ($3d^4$-$3d^4$) and Mn^{2+}-Mn^{4+} ($3d^5$-$3d^3$) pairs. The static JT distortion (present only for $x=0$) will act to stabilize the Mn^{3+}-Mn^{3+} complex by a few tenths of an eV, while the energy of the $3d^5$-$3d^3$ configuration may be lowered significantly by Hund's rule exchange. The stability of the $3d^5$-$3d^3$ complex could be limited by the 30% larger size[19] of the Mn^{2+} ion relative to that of Mn^{3+}, leading to non-negligible lattice strain energy (in comparison, Mn^{4+} ions are 20% smaller than Mn^{3+} ions). An examination of chemical Gibb's free energies of MnO, Mn_2O_3, and MnO_2 also indicates that the $3d^4$ configuration is significantly less stable than either $3d^5$ or $3d^3$ ions.[20] CD is not uncommon amongst JT-active d^4 and d^9 transition-metal-oxide (TMO) compounds; it has been observed in $La_{1-x}Ca_xCoO_3$, Mn_3O_4, $CaFeO_3$, $Sr_{1-x}La_xFeO_3$, and $Sr_2LaFe_3O_8$.[21] The atomic-structure effects that lead to CD also manifest themselves in the nonmonotonic progression exhibited by TMO ionic radii across the $3d$ series.[19] Valence instability effects may also account for the anomalously large dT_C/dP values observed in the CMR compounds,[22] and it could be involved in the CMR effect observed in the europium chalcogenides.[23]

To formulate a CD-based transport model, the relative Mn valence concentration must be specified. TGA results[16] are consistent with valence-specific Mn concentrations given by

$$[Mn^{2+}]=\xi-2\delta,$$

$$[Mn^{3+}]=1+2\delta-x-2\xi, \tag{6}$$

and

$$[Mn^{4+}]=x+\xi.$$

The x-dependent disproportionation coefficient ξ is a relative measure of the amount of 2+ and 4+ Mn that evolves from disproportionating Mn^{3+}-Mn^{3+} pairs. TGA measurements indicate that 70–80 % of the Mn^{3+} ions undergo CD for $x=0$ [$\xi(0)=0.4$], while the $3d^4$ configuration is fully stabilized by 45% divalent doping [$\xi(0.45)=0$]; ξ varies linearly with x between these extremes.[16] Electron hopping between 2+/3+ states is rarely observed, relative to the more frequent 4+/3+ hole hopping.[21] This is because the characteristic small polar hopping energy is determined, in part, by the difference in bond lengths between the initial and final configuration oxidation states; the 50% larger ionic size difference between 2+/3+ Mn ions relative to that of 3+/4+ indicates that, while 2+/3+ electron hopping will occur, it will do so at a considerable lower rate than that of hole hopping between 3+/4+ Mn sites. Hence, Mn^{2+} sites can be assumed to act as blocking sites for polaron transport. Within this model the fraction hole concentration is given by

$$c_h=\frac{[Mn^{4+}]}{[Mn^{4+}]+[Mn^{3+}]}=\frac{x+\xi}{1+2\delta-\xi}. \tag{7}$$

The $S_{c,\infty}(x)$ prediction based on the model [employing the Heikes expression, Eq. (5)] produces the solid line in Fig. 2 (assuming $\delta=0$); the prediction when the sample-specific excess oxygen level is accounted for are plotted as open triangles. This CD model provides excellent agreement with the experimental trend evident in the TEP data. The doping dependence of δ and ξ combine to produce a fractional hole concentration that is never far from 1/2 , and is only weakly x dependent.

In the CD-based transport model, the doping-dependent resistivity trend evident in Fig. 1(a) cannot be ascribed to an increase in holes because TGA measurements suggest that $[Mn^{4+}]$ is a slowly varying function of x due to the interplay between cation doping and charge disproportionation. Instead $\rho(x)$ is controlled by the rapid decrease in transport-inactive Mn^{2+} sites that occurs with increased divalent doping concentrations. Within a CD description, the FM insulator-FM metal phase boundary occurs at $x\approx 0.2$ because a 3D percolation path of hole-accessible Mn^{3+} transport sites exists only at and above this doping concentration. Spectroscopic evidence is needed to confirm that Mn^{3+} CD occurs in $La_{1-x}Ca_xMnO_{3+\delta}$, although lifetime effects could make this problematic.[24] The effect should be most pronounced at high temperatures where TGA measurements have been carried out.[16]

In summary, temperature- and doping-dependent TEP and resistivity measurements on $La_{1-x}Ca_xMnO_{3+\delta}$ indicate that transport above T_C involves small polaron hopping. The magnitude of S is too small to be accounted for by a simple $Mn^{3+/4+}$ nominal valence description. The data indicate that there are considerably more holes and/or fewer active Mn transport sites than expected. A charge disproportionation model based on the instability of the Mn^{3+} state relative to that of a Mn^{2+}-Mn^{4+} complex provides excellent agreement with the doping-dependent trends exhibited by both the TEP and the resistivity. These results provide a framework for future studies that examine the novel behavior exhibited by CMR compounds.

The authors thank A. Bishop, D. Emin, F. Garzon, R. Heffner, R. Lemons, H. Röder, M. Salamon, J. Thompson, S. Trugman, J. Zaanen, and J. Zang for illuminating discussions and encouragement. This work was performed under the auspices of the U.S. Department of Energy.

[1] G. H. Jonker and J. H. Van Santen, Physica **16**, 337 (1950); **16**, 599 (1950); E. O. Wollan and W. C. Koehler, Phys. Rev. **100**, 545 (1955).

[2] J. Volger, Physica **20**, 49 (1954).

[3] C. Zener, Phys. Rev. **82**, 403 (1951); P. W. Anderson and H. Hasegawa, *ibid.* **100**, 675 (1955); P. G. deGennes, *ibid.* **118**, 1412 (1960).

[4] R. M. Kusters *et al.*, Physica B **155**, 362 (1989); K. Chahara *et al.*, Appl. Phys. Lett. **63**, 1990 (1993); R. von Helmolt *et al.*, Phys. Rev. Lett. **71**, 2331 (1993).

[5] A. J. Millis *et al.*, Phys. Rev. Lett. **75**, 5144 (1995).

[6] D. Emin *et al.*, Phys. Rev. B **35**, 641 (1987); H. Röder *et al.*, Phys. Rev. Lett. **76**, 1356 (1986).

[7] M. F. Hundley *et al.*, Appl. Phys. Lett. **67**, 860 (1995); R. H. Heffner *et al.*, Phys. Rev. Lett. **77**, 1869 (1996); M. F. Hundley *et al.*, J. Appl. Phys. **79**, 4535 (1996).

[8] Prior TEP publications have focused on qualitative aspects of this transport effect in CMR systems. See R. Mahendiran *et al.*, Solid State Commun. **98**, 701 (1996); Baoxing Chen *et al.*, Phys. Rev. B **53**, 5094 (1996); J. Fontcuberta *et al.*, Appl. Phys. Lett. **68**, 2288 (1996); V. Crespi *et al.*, Phys. Rev. B **53**, 14 303 (1996); J.-S. Zhou *et al.*, Nature **381**, 770 (1996).

[9] P. Nagels, in *The Hall Effect and its Applications*, edited by C. L. Chien and C. P. Westgate (Plenum, New York, 1980), p. 253.

[10] M. Jamie *et al.*, Appl. Phys. Lett. **68**, 1576 (1996); T. T. M. Palstra *et al.* (unpublished).

[11] R. Mahendiran *et al.*, Phys. Rev. B **54**, 9604R (1996).

[12] D. Emin, Phys. Rev. Lett. **35**, 882 (1975).

[13] R. R. Heikes, in *Transition Metal Compounds*, edited by E. R. Schatz (Gordon and Breach, New York, 1963), p. 1.

[14] S_∞ will be somewhere between the constant term a_1 and the experimental high-temperature value S(325 K) because the Heikes term evolves from both low-T terms, not solely from a_1. Therefore, S_∞ was determined by taking the average of a_1 and S(325 K); this produces a maximum uncertainty of ± 20 μV/K in $S_{c,\infty}$ for $x>0$.

[15] The fact that this simple fit describes the TEP data above T_C indicates that temperature-dependent bandwidth effects are not present.

[16] J. W. Stevenson *et al.*, J. Solid State Chem. **102**, 175 (1993); J. A. M. Van Roosmalen *et al.*, *ibid.* **110**, 109 (1994); **110**, 113 (1994).

[17] A. Asamitsu *et al.*, Phys. Rev. B **53**, 2952R (1996).

[18] D. Emin (unpublished).

[19] R. Shannon, Acta Crystallogr. A **23**, 751 (1976).

[20] *CRC Handbook of Chemistry and Physics*, edited by R. C. Weast (CRC Press, Boca Raton, 1988), p. D-74.

[21] S. R. Sehlin *et al.*, Phys. Rev. B **52**, 11 681 (1995), and refer-

ences therein; P. D. Battle *et al.*, J. Solid State Chem. **77**, 124 (1988).

[22] J. J. Neumeier *et al.*, Phys. Rev. B **52**, 7006R (1995).

[23] S. von Molnar and S. Methfessel, J. Appl. Phys. **38**, 959 (1967); M. R. Oliver *et al.*, Phys. Rev. B **5**, 1078 (1972).

[24] EPR measurements on $La_{1-x}Ca_xMnO_{3+\delta}$ detect no evidence for individual Mn ions of any valency (2+, 3+, or 4+). The spectra may instead reflect a time or spatial average of the Mn configuration due to the nonstatic nature of the hopping process. See S. B. Oseroff, *et al.*, Phys. Rev. B **53**, 6521 (1996).